

FINAL REPORT ON STRUCTURAL MODELING AND ANALYSIS DECEMBER 2010

Project 1606ACD
FY2010 Deliverable ID: 3
Chris Tanner and Dr. Robert Braun :: Georgia Institute of Technology

OVERVIEW

This document provides a summary of the structural and fluid-structural analysis that has been performed on membrane structures as they relate to inflatable aerodynamic decelerators (IADs). The finite element solver is introduced and described in detail, highlighting the capabilities that make it well suited for analysis of these types of structures. Structural verification of the structural solver is provided in the form of a conference paper and supplemental results. Some potential future structural analyses are identified to further verify that appropriate models are being used. Additionally, a coupling scheme has been identified that will conservatively transfer forces and deflections between dissimilar surface meshes. This scheme is code independent, permitting the coupling of arbitrary fluid and structural solvers. Some test cases are presented to demonstrate the capabilities and deficiencies of this coupling mechanism. Possibly solutions are presented to circumvent the deficiencies in the scheme. Finally, a fluid-structure interaction (FSI) framework providing loose coupling between arbitrary codes is explained.

STRUCTURAL ANALYSIS SUMMARY

Analysis Code Overview

Supersonic IADs, such as the tension cone and isotensoid concepts shown in Figure 1, are purposefully designed to carry tensile loads only, allowing them to be constructed from lightweight, deployable membrane materials (most commonly coated textiles).

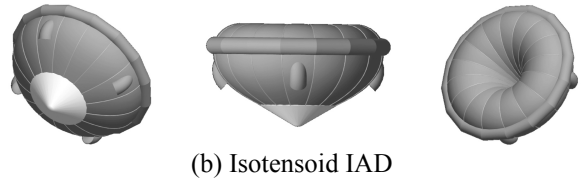


Figure 1. Supersonic inflatable aerodynamic decelerator configurations.

To analyze IADs, computational analysis was performed using the commercial code LS-DYNA. LS-DYNA performs nonlinear structural analysis using explicit time integration, in which position, velocity, and acceleration of each node is only a function of the node's state at the previous time step. Explicit integration eliminates a global stiffness matrix, which significantly reduces the memory requirements and computational cost of each iteration and adds robustness in the cases of ill-conditioned sparse stiffness matrices (as is often the case for membrane structures). Explicit analysis is less sensitive to machine precision and permits simpler element and contact formulations than implicit formulations. However, most explicit methods are only conditionally stable and require a relatively small timestep to ensure stability as determined by the Courant-Friedrichs-Lewy condition. Due to this timestep restriction, it is often necessary to compress the natural response time of a structure by applying loads or deflections at a higher rate to achieve timely results. To balance the increased internal and kinetic energy created by natural time compression, the response is often damped by artificially increasing the structure's mass. This type of natural time compression is not normally required using implicit analysis. Implicit structural analysis is generally well suited for static or modal analysis of well-behaved materials whereas explicit analysis is preferred for dynamic analysis or analysis of materials that exhibit discontinuous behavior. Due to the discontinuous behavior of membrane materials (such as textiles) around the zero stress condition, explicit methods are generally required for analysis of inflatable and membrane structures. All of the verification cases were solved using the double precision, symmetric multiprocessor version of the LS-DYNA version 971, release 4.2.

LS-DYNA was chosen over a research analysis code as it has mature material models and efficient finite element methods meant specifically for analysis of inflated structures, such as airbags. Additionally, its wide user base in the aerospace field lends familiarity and confidence in its solutions. Finally, construction of an FSI framework on widely used analysis tools increase the chance of the framework's utility outside of academia.

Model and Solver Description

Structural analyses use a membrane element that was specially formulated for use with inflatable structures. Implementation of the special element formulation occurs when the fabric material model is assigned to shell elements using a membrane formulation (ELFORM 5 or 9 in the SECTION_SHELL keyword). The membrane element is based on the Belytschko-Lin-Tsay element [1], which enables efficient analysis of large deflection, materially nonlinear shells by imbedding a corotational coordinate system in the element. Additional details regarding the constitutive formulation and limitations of the membrane element can be found in Sections 7 and 15 in Reference [2]. The fabric material model (MAT_FABRIC or MAT_034) is built upon a layered orthotropic composite material model, but is only valid for membrane elements. The fabric material model allows for the elimination of compressive stress in the associated element, allowing the element to buckle and/or collapse under compressive loads. This is typical behavior for a membrane and the option generally invoked (CSE 1). Discontinuous behavior near the zero stress condition is partially stabilized through the use of an artificial liner, which acts as a separate isotropic linear elastic material that augments the fabric's base material properties. This liner helps prevent crushed (zero volume) elements, but alters the fabric's stiffness in both tension and compression. Thus, a liner is recommended by LSTC at 10% the thickness of the base material and 10% of the base material's elastic modulus, effectively resulting in a 1% change in the stiffness parameter EA .

The fabric may be modeled as either isotropic or orthotropic with arbitrary fiber angles. Isotropic material definition requires one linear elastic modulus (E) and a Poisson's ratio (ν) with shear modulus (G) calculated by the relationship $G = 0.5E/(1 + \nu)$. Orthotropic material definition requires two independent linear elastic moduli in the warp and fill directions, a linear shear modulus, and a constant Poisson's ratio. The warp fiber direction is specified by an angle β ; the fill fiber can be specified to be any arbitrary angle with respect to the warp fiber (though warp and fill fibers are generally modeled as

orthogonal). Warp and fill fibers are modeled as separate layers of a composite material and not as a single layer of woven material, thus fiber reorientation while under shear is not modeled. Nonlinear elastic moduli curves can also be used if available. A diagram of a membrane element illustrating the imbedded coordinate system and fiber orientation angles is shown in Figure 2.

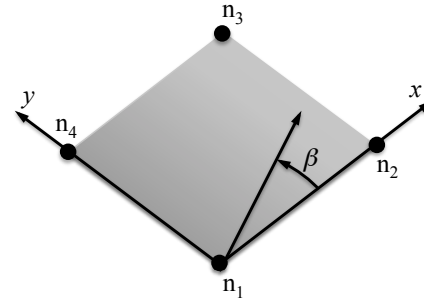


Figure 2. Shell element describing local coordinate system and fiber orientation.

Verification Summary

Analysis was performed on fundamental inflated membrane structures in order to verify proper modeling and code execution. Verification was accomplished by comparing computational results against static analytical solutions for three shapes: cylindrical column, torus, and a tension shell. A full description of the verification effort for inflated structures relevant to the tension cone IAD is given in Ref [3]. A brief summary of the document is given here highlighting some of the major findings and conclusions.

In general, LS-DYNA agreed very well with analytical theories for inflated structures. However, stress analysis of doubly curved surfaces, such as toroids and tension shells, was found to be insufficient to predict accurate behavior using linear theory. For toroids, ratios of major radius to minor radius are too large to use linear theory for current tension cone designs. For tension shells, material elasticity is not accounted for in the theory but was shown to significantly influence the circumferential stress distribution. Thus linear theory is only recovered in the limit as the tension shell load goes to zero.

Buckling and wrinkling behavior of inflated columns were analyzed and shown to agree with theory. However, LS-DYNA implements a non-physical "liner" that adds some compression strength to its membrane elements in order to help with stability. This liner was shown to significantly influence the solution when a configuration is in a wrinkled state. Thus, a solution may require the use of a liner for stability, but

it must be carefully implemented in order to avoid skewing the solution.

Some additional work was performed post publication of the referenced conference paper. Column buckling analysis was performed using an orthotropic material definition to observe differences in the buckling behavior. An orthotropic material definition was swapped into the column buckling finite element model in which the warp fibers were aligned with the column axis. Shear modulus was decreased by approximately 95% from the isotropic definition, which more closely corresponds to the measured shear modulus for the Kevlar material. Orthotropic analysis in LS-DYNA is complicated slightly by the presence of four separate membrane formulations, defined in Table 1.

Table 1. LS-DYNA orthotropic membrane formulations for fabric material [2]. All listed forms assume orthogonal fiber orientation.

Form	Description
0	Default; least costly; reliable
1	Invariant local membrane coordinate system
2	Green-Lagrange strain formulation
12	Update to Form 2

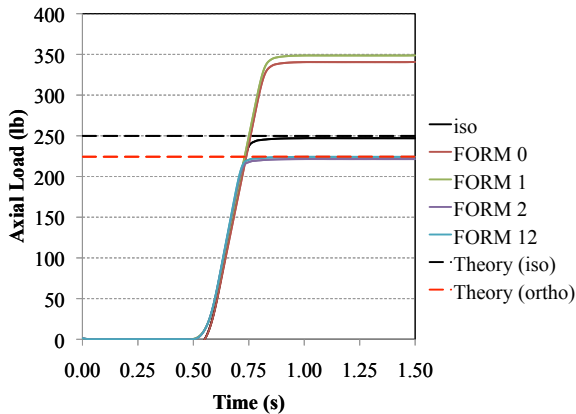


Figure 3. Comparison of buckling loads between various orthotropic membrane formulations.

Figure 3 illustrates the column buckling loads predicted by LS-DYNA for four different orthotropic material formulations. Fichter's theory [4] predicts a 10% decrease in the buckling load due to the change in shear modulus. Membrane formulations 0 and 1 result in a buckling load that is approximately 50% greater than predicted by Fichter. Membrane formulations 2 and 12 are both within approximately 1% of Fichter's solution, with form 12 resulting in almost an exact recovery of Fichter's prediction. These solutions bring two important aspects of orthotropic analysis to light. First, a 95% change in shear modulus causes only a 10% change in the predicted buckling load in a highly

inflated column. This suggests that orthotropic analysis may not be necessary, depending on the desired accuracy relative to model setup time. Second, orthotropic solutions in LS-DYNA must be prefaced by the assumed membrane formulation since the choice of this formulation appears to have a significant effect on the solution.

Future Work

Although an extensive effort has been completed to verify the accuracy and performance of LS-DYNA and its application to IADs, other cases can provide additional insight. The effects of orthotropic materials are still not well understood as implemented in LS-DYNA, in particular their effect on more complex structures (such as toroids) and the effect of fiber bias angle. Traditional construction patterns will use either "block" or "bias" orientation, shown in Figure 4. Which orientation is used depends on the desired structural characteristics, making fiber orientation a critical parameter for textile part fabrication.

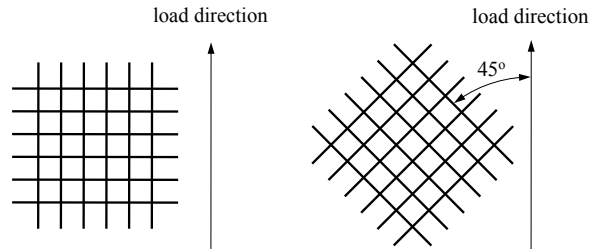


Figure 4. Fiber orientations used in construction of textile structures.

Three analyses are proposed to address concerns related to orthotropic materials. First, a faceted tension shell will be analyzed using isotropic and orthotropic material properties (both block and bias orientations). Results from these analyses will be compared to determine if stress distributions or deflections change significantly between the different models and fiber orientations for relevant tension shell sizes and pressure distributions. Second, stress differences observed from the tension shell comparison will be compared against strength data for relevant textile materials, such as Kevlar and Vectran. If differences in the analyses are greater than 20% of the strength of a given material, then the behavior of orthotropic materials is significant and should be performed despite the increased model complexity. Third, a faceted torus will undergo buckling analysis using both isotropic and orthotropic materials at various internal pressures. The goal of this analysis is not to compare against theory, but to compare one analysis against the other to understand the relative differences between the two material models. Loading at various internal pressures will

provide additional data regarding the role of pressure in orthotropic analysis.

DATA TRANSFER BETWEEN DISSIMILAR MESHES

Fluid analysis and structural analysis have distinctly different grid requirements in order to produce sufficiently accurate and timely results. For example, the aerodynamics surface grid may consist strictly of triangles and be very dense where the structural grid may consist of strictly quadrilaterals and be significantly less dense.

Thus, in order to perform fluid-structure interaction (FSI) analyses, it is necessary to provide a mechanism to communicate data between the two grids. In particular, forces due to aerodynamic pressure need to be transferred from the aerodynamic grid to the structural grid and deflection due to structural response needs to be transferred from the structural grid to the aerodynamic grid. Samareh [4] developed code to interpolate and transfer forces, moments, and deflections between dissimilar grids for FSI applications. The algorithm uses the inverse isoparametric mapping (IIM) method, where an isoparametric element uses the same shape functions to interpolate data between the two grids. A slight modification to the IIM method mathematically guarantees the conservation of forces and moments. As the aerodynamic grid and the structural grid may not necessarily lie on the same surface or be of the same shape, data must be projected from one grid to the other (e.g. lift forces on a wing projected onto a beam element representation of the wing). A simple pre/post-processor can make the discrete data transfer tool compatible with any fluid and structural solver file format.

Figure 5 shows an example axisymmetric tension shell case exhibiting some distinct differences between the aerodynamic and structural grids. The structural grid (orange lines, left) is significantly less dense than the aerodynamic grid the tension shell is modeled as a single surface with no physical thickness. In contrast, the aerodynamic grid has a tension shell that must be modeled with a finite thickness to properly define the computational volume grid. Additionally, there are fillets between the tension shell and torus and tension shell and backshell to provide a smooth, transitional surface to create a good quality volume grid. Finally, the structural model uses a complete torus to properly model the behavior of a pressure-stabilized torus where as the torus in the aerodynamics grid is truncated at the fillet. Although these differences appear minor in Figure 5, they will create issues as will be shown later.

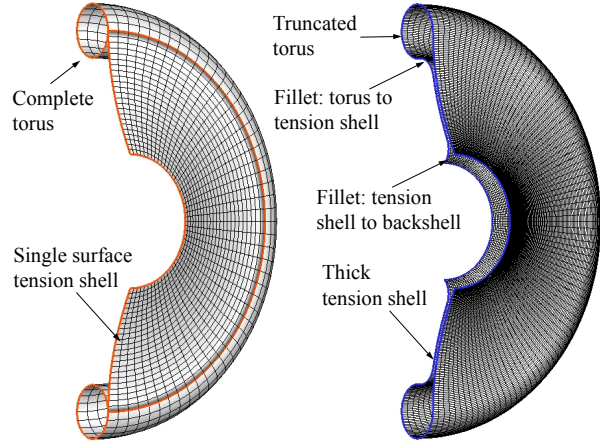
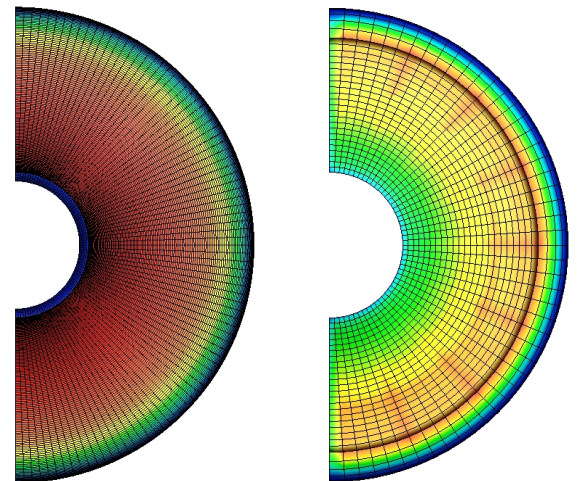
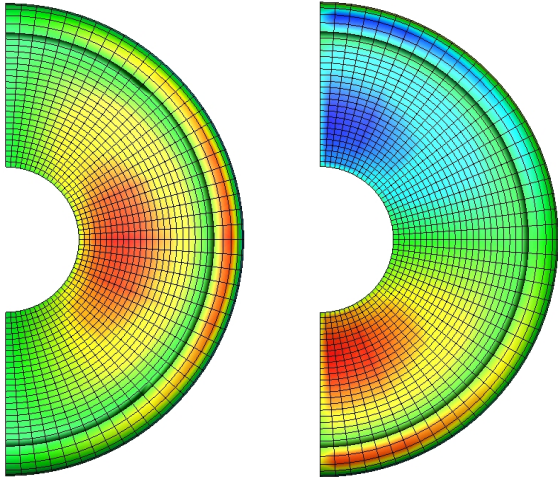


Figure 5. Comparison of structural grid (left, orange) and aerodynamic grid (right, blue) illustrating modeling differences.

Pressure data was obtained using the computational fluid dynamics code FUN3D for the as-designed axisymmetric tension shell shape for a flight condition at Mach 2.5 and 0° angle of attack. The discrete data transfer (DDT) tool developed by Samareh was then used to transform pressure data into force data and interpolate it to the structural grid. Figure 6 shows the pressure distribution on the aerodynamic grid and the resulting force distribution in the x, y, and z directions. These results show an appropriate symmetric force distribution corresponding to an axisymmetric pressure field.



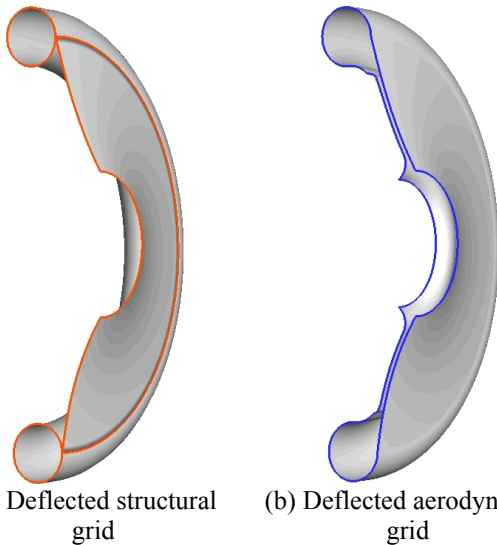
(a) Contours of pressure coefficient on aero grid (b) Contours of x-force on structural grid



(c) Contours of y -force on structural grid (d) Contours of z -force on structural grid

Figure 6. Contours of pressure and force data on a tension shell.

A finite element simulation was performed using the force distribution show above using a rigid torus. The tension shell deflected axially and these deflections were transferred back to the aerodynamic grid using the DDT tool. Figure 7 shows the results of the deflection transfer.



(a) Deflected structural grid (b) Deflected aerodynamic grid

Figure 7. Results of deflection transfer from structural grid to aerodynamic grid.

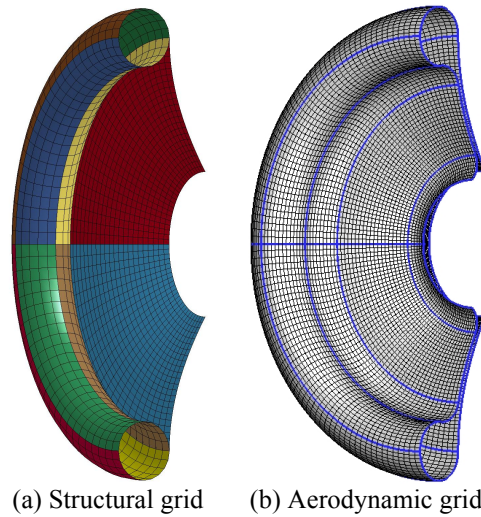
Transfer of deflections to the aerodynamic grid resulted in staircasing of the surface and severe surface element distortion at the torus-tension shell fillet. The fluid solver (FUN3D) has the ability to deform and adapt the volume mesh to a new surface geometry; however, the element distortion in the fillet region was too great for the automatic deformation routines. In order for loosely-coupled FSI to occur in a timely manner, it is

imperative that the fluid solver be able to automatically adapt the volume grid. Thus, a solution must be found to prevent such extreme element distortion. Although not shown, several fillet sizes were tested and all resulted in staircasing and element distortion.

The IIM method of transferring discrete data was shown by Smith et. al. [5] to be very good at data interpolation, but less accurate at data extrapolation. The geometric distortion at the fillet is likely due to extrapolation that the DDT routine must perform in order to transfer the deflection from the structural grid to the aerodynamic grid. Odd behavior such as this did not manifest during the aerodynamic to structural data transfer, as data was only interpolation was being performed.

Future Work

Three potential solutions are being explored to remedy the problems encountered during structural to aerodynamics data transfer. The first solution involves dividing the geometry up into sections manually, as shown in Figure 8, specifying which surfaces are to exchange data (instead of specifying each grid as just one body). Manually specifying which data is to be interpolated and extrapolated may help decrease the geometric distortions witnessed in Figure 7.



(a) Structural grid (b) Aerodynamic grid

Figure 8. Grids divided into sections for better data transfer.

A second solution involves creating a fillet on structural grid similar to the aerodynamic grid. This will provide a new surface that should minimize the amount of extrapolation performed by the DDT routine. However, a new component on the structural grid may change the load paths and alter the structural response of the tension shell. It is hoped that the use of contact algorithms with very low friction coefficients and

materials with low elastic moduli will minimize the structural impact of these new components.

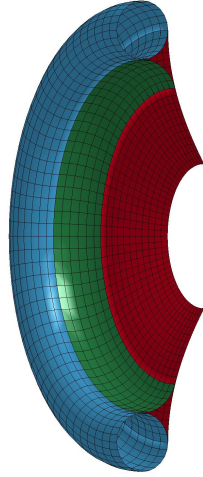


Figure 9. Structural geometry modified to include non-structural fillet.

A third solution involves departing from the IIM method for geometry deformation and developing a new method based on non-uniform rational B-splines (NURBS). The primary advantage of this method is that the geometry will always be smooth. However, there are many technical hurdles along this development path. Smith et. al [5] utilized a form of this method, but in 2D only -- the method would have to be extended to 3D before becoming useful. Additionally, discretization of a NURBS surface is considerably easier to accomplish than creating a NURBS definition from a discretized surface (the latter would be needed to transfer deflection data). A NURBS surface can be obtained from a discretized surface using least squares fitting methods, but these methods can be computationally intensive and can result in several equivalent, non-unique solutions. Finally, the surface mapping would not be exact every time as there is always some amount of error associated with a least-squares fitting process. Nevertheless, the method is attractive and, based on a thorough literature search, has not been implemented in 3D in any application.

FSI FRAMEWORK DESCRIPTION

Coupling between fluid and structural solvers can be performed on essentially three levels, each requiring distinctly different frameworks to enable FSI analyses.

Strong coupling (also called monolithic coupling) ideally involves simultaneously solving a single large system of nonlinear equations containing terms for fluid behavior (\mathbf{U}_1) and structural behavior (\mathbf{U}_2). This

coupling can be represented mathematically by the implicit system in Equation 1

$$\begin{bmatrix} \mathbf{U}_1 \\ \mathbf{r}_T \end{bmatrix}^n = \mathbf{A} \cdot \begin{bmatrix} \mathbf{U}_1 \\ \mathbf{r}_T \end{bmatrix}^{n+1} \quad (1)$$

where \mathbf{A} is a square matrix and n is the current time step. However, developing a monolithic set of equations that can be solved efficiently can be very difficult and coupling will have to be performed on the code level. Additionally, the entire system must evolve at the same rate, which may require very small timesteps or some averaging of high-frequency behavior. Strong coupling will be necessary to efficiently capture dynamic aeroelastic behavior on small timescales with high time accuracy.

Tandem coupling simplifies the coupling process, but must be implemented on the code level similar to the monolithic method. This method involves solving the fluid and structural systems separate, but integrating them forward in time simultaneously. The two systems contain a cross-term that exchanges information between the systems explicitly at each time step. This coupling can be represented by the system in Equation 2

$$\begin{aligned} \mathbf{U}_1^{n+1} &= F[\mathbf{U}_1^{n+1}, \mathbf{C}_2^n] \\ \mathbf{U}_2^{n+1} &= F[\mathbf{U}_2^{n+1}, \mathbf{C}_1^n] \end{aligned} \quad (2)$$

where \mathbf{C}_1 is the aerodynamic cross-term vector and \mathbf{C}_2 is the structural cross-term vector. Tandem coupling can capture static and some dynamic behavior but may require more computation time to converge. Additionally, tandem coupling solutions are typically energy-increasing and less time accurate than monolithic methods. Time accuracy and energy increase can be minimize by implementing a serial staggered iteration scheme as proposed by Lesoinne and Farhat [6] and shown in Equation 3 and Figure 10. However, improved accuracy comes at the expense of computation time.

$$\begin{aligned} \mathbf{U}_1^{n+1/2} &= F[\mathbf{U}_1^{n-1/2}, \mathbf{C}_2^n] \\ \mathbf{U}_2^{n+1} &= F[\mathbf{U}_2^n, \mathbf{C}_1^{n+1/2}] \end{aligned} \quad (3)$$

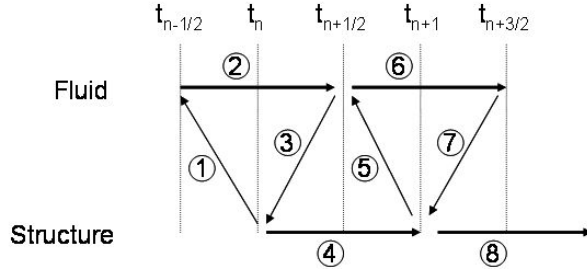


Figure 10. Diagram of improved serial stagger method [7].

Weak coupling is the simplest method to implement and requires very little, if any code development. Two independent solvers are used and coupled externally through a data translation and transfer mechanism. The weak coupling formulation in Equation 4 appears very similar to tandem coupling except that cross-terms are not necessarily exchanged at every time step.

$$\begin{aligned} \mathbf{U}_1^{n+1} &= F[\mathbf{U}_1^{n+1}, \mathbf{C}_2] \\ \mathbf{U}_2^{n+1} &= F[\mathbf{U}_2^{n+1}, \mathbf{C}_1] \end{aligned} \quad (4)$$

This method can be the easiest to implement and can efficiently provide solutions to static aeroelastic or large timescale problems. Additionally, it affords the analyst the ability to select their preferred aerodynamic and structural solvers and implement them together without any modification to their source code. Thus, weak coupling is the preferred method for most preliminary and design-oriented engineering analysis.

For its ease of implementation, ability to use arbitrary solvers, and applicability to most industrial analysis, a weak coupling method was selected as the FSI framework for this research. In this framework, surface pressures are obtained by computational fluid dynamic analysis using the FUN3D Navier-Stokes solver developed by NASA Langley Research Center. This particular flow solver has specific functionality for static aeroelastic analysis such as grid adaptation and grid deformation routines. Pressure data is transferred from FUN3D through the discrete data transfer tool (described in the previous section) and written as prescribed loads on a structured LS-DYNA grid. Deflections obtained from the structural analysis are transferred through the discrete data transfer tool to the unstructured aerodynamics grid and FUN3D adapts the volume mesh to the new shape. This process, shown in Figure 11, is iterated upon until convergence.

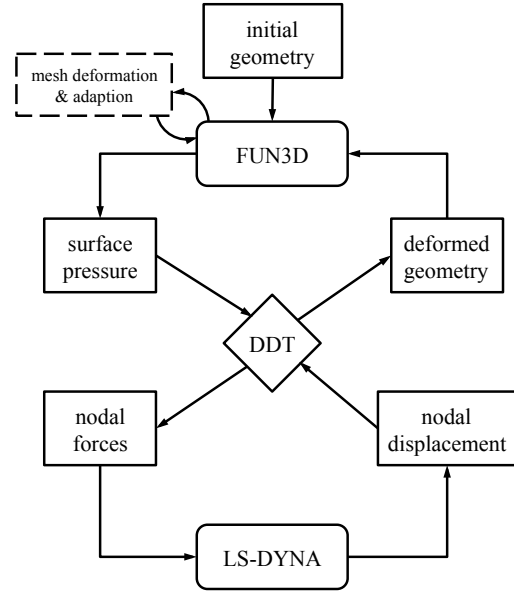


Figure 11. FSI framework diagram.

Implementation of this framework has already begun. File input/output and code execution can be scheduled using a cluster queuing system to allow for unattended operation of the framework across multiple computing nodes.

REFERENCES

- [1] Belytschko, T., Lin, J., Tasy, C., "Explicit Algorithms for the Nonlinear Dynamics of Shells," *Computer Methods in Applied Mechanics and Engineering*, vol 42, pp. 225-251, 1984.
- [2] LSTC Corporation, *LS-DYNA Keyword User's Manual*, Volume I and II, Version 971, May 2007.
- [3] Tanner, C., Cruz, J., Braun, R., "Structural Verification and Modeling of a Tension Cone Inflatable Aerodynamic Decelerator," *AIAA / ASME / ASCE / AHS / ASC Structures, Structural Dynamics, and Materials Conference*, AIAA 2010-2830, April 2010.
- [4] Fichter, W. B., "A Theory for Inflatable Thin-Wall Cylindrical Beams," NASA TN D-3466, June 1966.
- [4] Samareh, J., "Discrete Data Transfer Technique for Fluid-Structure Interaction," *AIAA Computational Fluid Dynamics Conference*, AIAA 2007-4309, Jun 2007.
- [5] Smith, M. J., Hodges, D. H., Cesnik, C. E. S., "An Evaluation of Computational Algorithms to Interface Between CFD and CSD Methodologies," WL-TR-96-3055, November 1995.

[6] Lesoinne, M., Farhat, C., “Higher-Order Subiteration-Free Staggered Algorithm for Nonlinear Transient Aeroelastic Problems,” *AIAA Journal*, Vol. 36, No. 9, pp. 1754-1757, May 2006.

[7] Rohrschneider, R. R., “Variable-Fidelity Hypersonic Aeroelastic Analysis of Thin-Film Ballutes for Aerocapture,” Ph.D. Thesis, Georgia Institute of Technology, April 2007.